STREAM

IST-1999-10341

STREAM consortium: CNR-LAMEL/ST-MICROELECTRONICS/UNIVERSITY OF SHEFFIELD/ISEN/SOFT IMAGING SYSTEM/UNIVERSITY OF PERUGIA/IMEC/CNR-IESS

Deliverable
Work package nr. 3

Partners: **CNR-LAMEL, ST, SIS**
USFD, IMEC, CNR-IESS

Coordinator: **CNR-LAMEL**

DELIVERABLE D6
Theoretical and experimental study of the effects of the different optical parameters and lenses on the spatial resolution of the Raman system

Main author:	Ingrid De Wolf		
Contributing Author(s):	Merlijn van Spengen (IMEC)		
Date:	03 - 07 - 2000	***Doc. No:***	IST10341-IM-RP001
Keywords:	Raman spectroscopy, spatial resolution		
Distribution list:	B. Netange (EC), A. Armigliato, G. Carnevale, V. Senez, T. Schilling, A.G. Cullis, I. De Wolf, S. Lagimarsino, G. Carlotti,		

Table of contents

Abstract

Micro-Raman spectroscopy is a well known technique that can be applied for the measurement of local stresses in semiconductor devices. A drawback of this technique is that the spatial resolution of a common instrument is, at best, about 1 µm.
In this deliverable we report on the theoretical calculations and experiments which were performed to improve the spatial resolution of micro-Raman spectroscopy. A minimal spot size of 0.3 µm was obtained.

1 Introduction

1.1 Raman instrumentation

The increasing densification and miniaturisation of devices in microelectronics components demands analytical techniques with a very high spatial resolution, in general higher than the limit set by far field diffraction of visible light. This offers a problem for optical techniques, such as micro-Raman spectroscopy (µRS). µRS takes an important place for the measurement of local mechanical stress. In this technique, the light beam of a laser is focused through an optical microscope on the sample. The scattered light is collected through the same microscope and directed into a spectrometer, and send to a CCD detector, to analyse the spectrum. A typical Raman instrument is shown in Fig. 1. It is clear that this is a rather complex optical instrument.

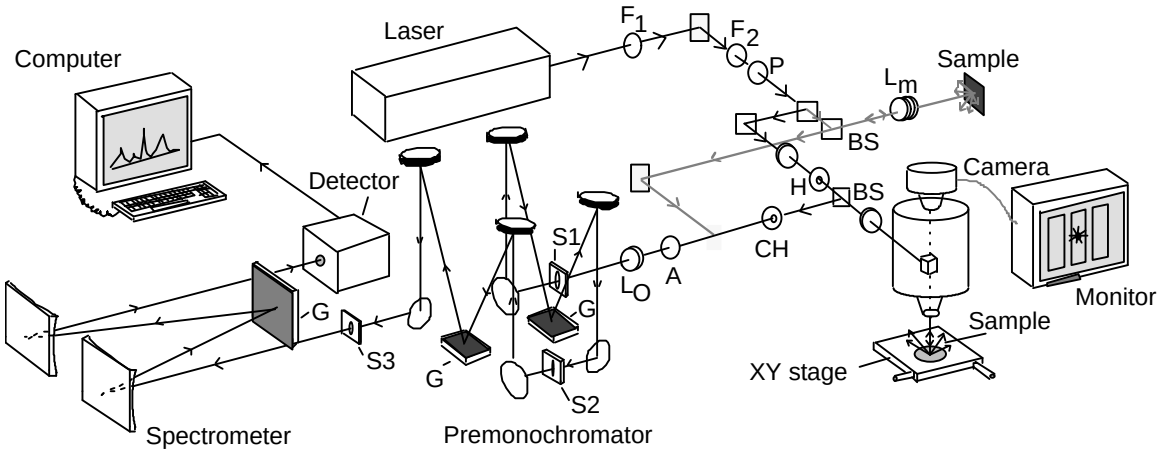

Figure 1- *Typical Raman spectroscopy instrument with micro (microscope) and macro (lens Lm) option. Including filters (F), polariser (P) and analyser (A), beam splitters (BS), pin holes (H) and confocal hole (CH), scrabler (Lo), slits (S) and gratings (G).*

The light (photons) interacts with the lattice vibrations (phonons) of the sample. The scattered light contains frequency components (Raman peaks) which have a frequency equal to the one of the lattice vibrations. Figure 2 shows a typical Raman spectrum of crystalline Si. Also the sharp, Gaussian-like plasma lines of the argon laser, which can be used for calibration, are visible.

Micro-Raman spectroscopy suffers from a too large probing beam spot when compared to the dimensions of current devices. The spatial resolution of a common micro-Raman spectroscopy instrument is about 1 µm. Up to now, three possible solutions were suggested to increase the resolution of micro-Raman spectroscopy: the use of near-field scanning optical microscopy (NSOM) [1-4], the use of a UV micro-Raman spectroscopy instrument (UV-µRS) [5], and the use of a solid immersion lens (SIL) [6].

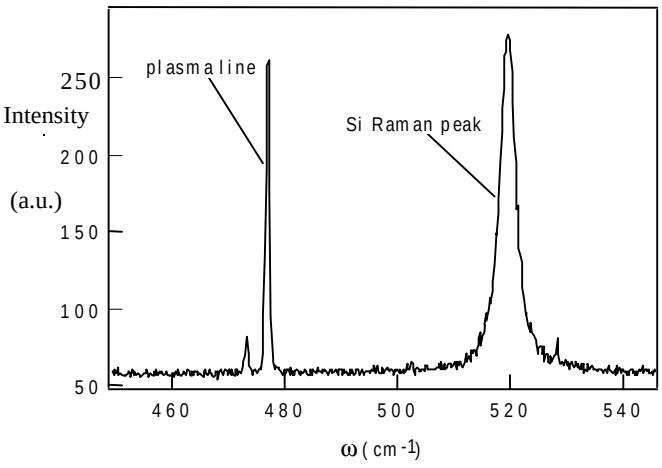

Figure 2 - *Raman spectrum of crystalline silicon, measured using the 457.8 nm line of an argon laser. It shows the Si Raman peak and plasma lines from the laser.*

1.2 Spot size considerations

The spatial resolution of a Raman instrument is mainly defined by the size of the focused laser spot on the sample. In order to define the spatial resolution, one should first define the 'spot size' of a focused laser beam. A very useful definition of the spot size is given by defining the diameter of a *diffraction limited* spot to be the diameter at which the intensity of the spot has decreased to $1/e^2$ of its value in the middle of the spot. This kind of spot is obtained by having a laser beam with a diameter much larger than the entrance aperture of the focusing lens (uniform illumination) and is the smallest spot we can ever obtain with ordinary optics. It has an intensity profile of the form

$$I(r) = I(0)\left[\frac{2J_1(r)}{r}\right]^2$$

with $J_1(r)$ a Bessel function of the first kind of order one, and r the distance to the middle of the spot [10,11]. The Rayleigh criterion

$$r = \frac{1.22\,l}{2NA}$$

gives us the radius of the ring at which the first zero of the Bessel function occurs, where λ is the wavelength of the light, and NA the numerical aperture of the objective. The diffraction limited spot reaches its $1/e^2$ intensity value at the little smaller radius

$$r = \frac{0.88\,l}{2NA}$$

so its diameter is given by

$$\varnothing = \frac{0.88\,l}{NA} \qquad (1)$$

This is the fundamental minimum spot size. When the laser beam is smaller and the aperture is not completely filled, the spot is larger and approaches a Gaussian distribution [12]. The numerical aperture of the objective consist of two terms as given in

$$NA = n_i \sin(\theta) \qquad (2)$$

The angle θ is the angle the outer rays make with the optical axis, and n is the refractive index of the material surrounding the object.
One can see from Eq. 1 that one can do two things to improve the resolution: use a shorter wavelength, and use a higher NA. Ordinary objectives (with a sample in air) are limited with $n_i = 1$ (refractive index of air) to a maximum NA ≈ 1 ($\sin\theta \leq 1$ always).

1.3 Near field Scanning Optical Microscopy (NSOM)

The Raman imaging capabilities in NSOM were shown to work for materials with high Raman scattering cross sections, such as diamond. However, the sensitivity of NSOM Raman spectroscopy is very low: for silicon a sensitivity of about 1 photon per second was reported. This means that NSOM for Raman can only become of practical interest for analysis of microelectronics devices if larger near field tips (100 nm versus the current 20-50 nm), improved collection and transmission efficiency, resonant excitation, and detectors with higher sensitivity are used. Measurements of stress in silicon using NSOM were reported in [2]. However, because the intensity of the Si Raman peak was still small in these experiments (about 150 counts in [2]), the peak frequency can only be determined with an error of about ± 0.2 cm^{-1}. Assuming uniaxial stress, this corresponds with a stress value of ± 90 MPa [13]. With conventional µRS, shifts as small as 0.02 cm^{-1} can be measured, indicating a 10x better sensitivity for stress [13]. This sensitivity is certainly required for the investigation of local stress in microelectronics devices. However, the NSOM-Raman spectroscopy is very promising for the future. It can be expected that the sensitivity of NSOM-Raman will increase in future, when for example probe tips with a better collection efficiency and collecting mirrors are used. A disadvantage of NSOM is that it only works well if the distance between lens and sample is small enough to have near field conditions (see 1.6).

1.4 UV-µRS

The UV-µRS approach is very promising. Since the diameter of the focused laser beam depends directly on the wavelength of the laser light, a reduction of this wavelength from typically 514 nm used in conventional µRS to for example 240 nm, leads in theory to a reduction of the beam spot with a factor larger than two. In practice the UV-µRS reduction is smaller due to the lack of good objectives with high numerical aperture in the UV region. UV-µRS is used mainly for the investigation of stress very near the surface of a sample. The resolution of nowadays UV-Raman instruments is about 1 µm [6].

1.5 Other near-field solutions: the immersion lenses

Apart from NSOM and UV-μRS, there are two other near-field possibilities to improve the resolution, an oil immersion objective and a solid immersion lens (SIL). The oil immersion objective has been well known in biology for decades, but was only recently shown to be useful in micro-Raman experiments [14]. The second approach is to use a Solid State Immersion (SIL) lens in combination with near-field optics [8]. The SIL can be a hemisphere of glass (called the HSIL), or a ball lapped and polished from one side to a thickness of r(1+1/n), with r the radius of the ball and n its refractive index (called the Truncated (T-) SIL). The SIL lens was demonstrated to work very well for near-field optical data storage [7]. Also its application for photoluminescence imaging was discussed [9]. Studies are going on for the use of this lens for Raman spectroscopy [6]. The improvement in spot size over a normal objective is in both oil and solid immersion lens due to the immersion of the sample in a high refractive index material (the factor n_i in equation 2). This reduces the effective wavelength of the light because the frequency remains the same, while the light travels less fast.

The NA of a HSIL is given by $NA = n_{SIL} NA_{objective}$, the NA of the TSIL by $NA = n_{SIL}^2 NA_{objective}$, with a maximum of n_{SIL} [15].

This only works if the shortened wavelength is directly transferred to the sample. With the oil immersion lens, the shortened wavelength is directly transferred to the sample by the oil, in the case of a SIL, this is only the case if the SIL is directly on top of the sample. Because an air gap is always present, the shorter wavelength effect has to be transferred through the air gap by its exponentially decaying evanescent waves. The SIL therefore has to be in the close proximity of the sample. Even if the sample is clean, height differences may spoil the resolution. The SIL only works well if the distance between lens and sample is small enough to have near field conditions. This is possible on flat samples, but more difficult on structured samples. For the latter, special lenses with a small tip have to be developed [8]. The lenses which are at this moment available also suffer from abberation problems. Good focusing is only possible when the center of the lens is exactly above the structure on the sample which has to be measured. This means that the lens had to be connected to the microscope, in order to be able to perform a scan across a structure.

1.6 Conclusions

A drawback of both NSOM and SIL, is that they need near-field conditions. If the distance between probe tip or SIL lens and the sample is larger than about 100 nm, near-field conditions are not obtained. This is an important problem when one wants to apply these techniques to microelectronic structures. Indeed, structures such as for example LOCOS or STI (shallow trench isolation), have a silicon surface that either shows variations in topography larger than 100 nm, or where part of the surface is covered by oxide or nitride layers thicker than 100 nm. If want wants to monitor the local stress variations in these structures, SIL or NSOM can not be used. A possible solution could be to cleave the sample and to measure from the side, but cleaving might affect the local stresses.

In this report, we discuss alternative solutions to increase the resolution of the Raman spectroscopy instrument. We will discuss: the use of an autofocus system, an oil-immersion lens, and mathematical deconvolution.

2. Autofocus module

2.1 Introduction

In micro-Raman spectroscopy a laser beam is focused to a small spot on the sample through an optical microscope. In praxis, the focused spot turns out to be almost twice this theoretical limit, mainly for two reasons. As a first point, focusing of microscope objectives by an operator is never perfect, because of the small depth of focus of most used objectives. Even when the initial focus was right, the sample object can drift out of focus due to the movement associated with the scanning of the surface, temperature changes, etc. A second problem encountered is that the surfaces being investigated are never perfectly flat, and this spoils the maximum obtainable resolution as well. For the investigation of these devices, a perfect focusing is mandatory as a first step to have a good resolution.
To obtain the highest resolution, a dedicated micro-Raman spectroscopy auto-focus module was built in-home. A commercial system was available on the instrument, but it was not accurate enough for the purpose of high resolution measurements. Our system allows the microscope objective to be positioned, before the acquisition of a Raman spectrum, with 5 nm steps over a distance of 350 μm, thereby enabling the possibility to investigate samples even with very large height differences.

2.2 Working principle

The basic micro-Raman spectroscopy measurement system is given in fig. 3. To be able to automatically focus the objective, a partially reflecting mirror reflects a few percent of the light coming back from the sample through a pinhole onto a photo-detector. Auto-focusing is done by positioning the objective for maximum intensity, because the intensity of the reflected light is maximized when the objective is positioned in the exact focal plane.
To do that, a piezo positioner (PIFOC) is mounted between the objective and the microscope objective mount head. By applying a voltage to the piezo, the position of the objective relative to the sample can be changed. A block schematic of the electronics is given in fig. 4. A microcontroller communicates with the measurement PC and performs the auto-focus action. It reads in the voltage from the detector by means of an A/D converter, and is able to position the objective by setting a voltage on the D/A. This voltage is fed to a power amplifier provided by the PIFOC manufacturer. In this amplifier, a position control loop is integrated to correct for the hysteresis and the creep of the piezo positioner.

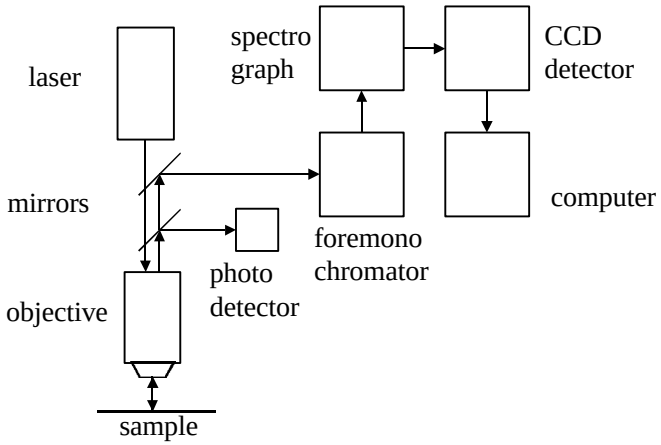

***Figure 3** - Raman system with beam splitter after the objective and photo detector, used for auto-focusing.*

When we move the objective through the focal plane, the intensity of the collected laser light will vary with the position as an asymmetrical Lorenz function [16]. The highest intensity is found at the focal plane, so the microcontroller module which is connected to the piezo only has to do the following procedure: (1) move the objective through its entire range, (2) record the intensity, and then (3) move back to the position at which the highest intensity was found. In praxis, the scan is performed first in a fast, rough way, and then again in slow 5 nm steps near the focal plane over a much smaller distance range. The module is triggered by the Raman spectroscope acquisition control computer just before a spectrum is acquired, and sends back the command to proceed when the focusing is done.

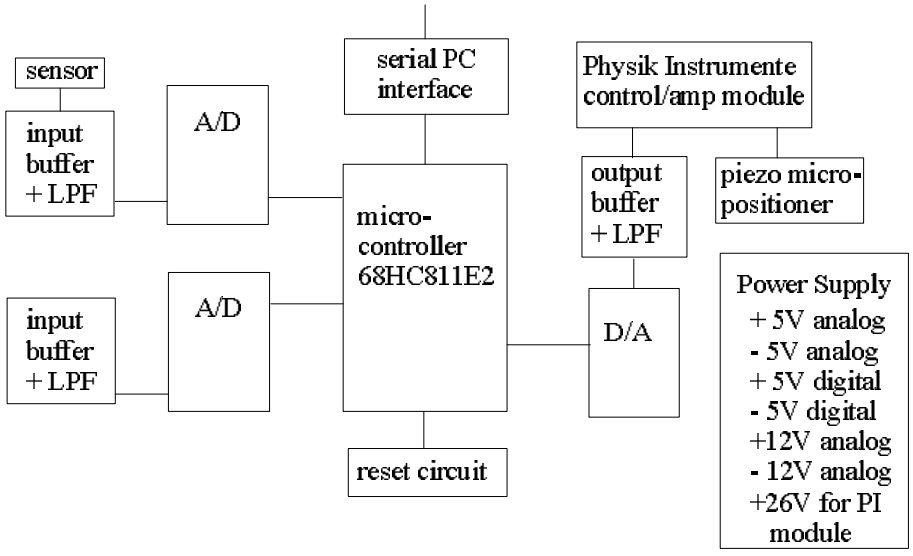

***Figure 4** - Block schematic of the auto-focus electronics.*

2.3 Detailed description of the actuator and control electronics

The heart of the electronic system is a Motorola MC68HC811E2 microcontroller, with 2kB of EEPROM, 256 bytes of RAM, a serial communications interface (RS232) for use with a host computer, and a serial peripherial interface (SPI) for communication with

other devices, such as A/D converters. One of the 16 bit A/D converters is used to sample the light intensity on the detector in the microscope, and a 16 bit D/A converter is coupled to the Physik Instrumente piezo steering module (E-610.L0). This module has a position control loop and generates the voltage for the microscope objective piezo positioner (PIFOC Physik Instrumente P-723.10). An RS232 serial interface is used for communication with the host PC. Special low noise operational amplifiers, a highly stable reference voltage generator and a lot of separated voltages and ground connections were used for low noise acquisition of the intensity signal.
The PIFOC objective positioner is a stack of piezoelectrically active crystals, all connected parallel, so that a relatively low voltage (100V) is enough to drive the positioner through its full 350 μm range. Furthermore, a LVDT (linear voltage differential transformer) position sensor is incorporated in the PIFOC. The PIFOC is very easily used: one just screws in an objective at one side, mounts it in the microscope objective head on the other side, and the setup is ready.
The LVDT sensor is very important, because a piezo crystal exhibits peculiar behavior when voltages are applied to it. Not only does it change shape (which is what we would like a position actuator to do), but it suffers from hysteresis and creep. The hysteresis manifests itself as the fact that the same voltage does not necessarily mean that the objective is always in the same position. This might be corrected for partly by always starting from the same position when focusing, but this does not prevent the creep from occurring. It means that after a step function-like voltage change is applied, the piezo does not immediately reach its final value. It will take several minutes before the piezo stops moving significantly.
For that reason, we cannot position the piezo by just applying a voltage to it, but we have to incorporate a control loop. Physik Instrumente provides sophisticated control electronics for this purpose, so an OEM version, to be built in with the microcontroller electronics, was obtained from them. This control electronics board also contains the power amp stage, which delivers the 100V the piezo needs. The input signal is a voltage which is converted to an absolute position of the objective. When we assume that the accuracy is determined by the D/A converter, we can calculate the minimal position change we can achieve. We used a 16 bit D/A converter, and hence we can position the objective in 2^{16} steps over 350 μm, resulting in a step size of $350\mu m/2^{16} \approx 5$ nm. It was found that noise in the system obscures the two least significant bits, and therefore the actual position is known to within 20 nm.
The application of a control loop preventing hysteresis and creep of the piezo was never before incorporated in an auto-focusing system for micro-Raman spectroscopy. However, this is really important for very high spatial resolution Raman imaging.

2.4 Software

When the sample is positioned under the microscope with an XY-stage at the location where a spectrum should be taken, the computer sends a “start” command to the auto-focus module. The microcontroller positions the objective in its lowest position and records the intensity of the reflected laser light falling on the photo-detector. In vertical steps of 0.2 μm, the intensity of the reflected light is compared to the highest previous value. If it is higher, the newly found highest intensity position is stored in the internal

RAM of the microcontroller. When the scan is finished, the objective is positioned a little below the found "best" position, and the scan is performed again over a much smaller distance (4 μm). This time, the scan is in 5 nm steps for maximum accuracy. There is a little delay loop between the points to ensure that the power amplifier/control system of Physik Instrumente does not "lag behind". After the scan, the objective is placed at the position where the highest intensity was found, and a "ready" command is sent back to the host computer.

3. Spot size - experimental results

3.1 Introduction

To find out which approach is the best for practical high spatial resolution micro-Raman spectroscopy, experiments were carried out with both an oil immersion objective and two solid immersion lenses (a TSIL and an HSIL).
The experiments were carried out with an XY-800 DILOR Raman spectroscopy system. The sample was mounted on an XY-stage, which allowed moving the sample in steps of 0.1 μm.
We first made sure that the oil itself does not give a Raman signal which could obstruct the Raman signal of silicon. Fig. 5 shows a typical Raman signal of (100) crystalline silicon, measured with the conventional lens (dotted line) and with the oil immersion lens (full line). In both spectra, the Si Raman peak is visible at 521 cm^{-1}, and also some plasma lines of the laser can be seen. We did not detect any Raman signal from the oil. Both experiments were performed using the same output power of the laser, 40 mW, but for the normal lens an integration time of 30 s was used, while for the oil-immersion lens, an integration time of only 10 s had to be used to obtain a similar Raman intensity. If the same integration time is used, the intensity of the Raman signal using the oil-immersion lens is about 3x larger than the intensity of the signal using the normal lens. This is a direct effect of the larger numerical aperture of the oil-immersion lens. The oil-immersion objectives admit a wider cone of rays than a dry objective with the same diameter would. For a dry objective, the cone of rays emerge from the silicon bulk into the air, and consequently are bent outwards by the refraction, the angular divergence being thus increased; in an oil-immersion objective on the other hand, this refraction is much smaller. So, using an oil lens, one obtains a 3x higher sensitivity. As a result, when a higher sensitivity is not required, as for c-Si which is a strong Raman scatterer, one can reduce the integration time with a factor three, meaning that the experimental measuring time can be shortened by the same factor.
In order to determine the spatial resolution of the lenses, a scan was performed across the edge of a $TiSi_2$ line on a (100) silicon substrate, with steps of 0.1 μm, starting on the line and ending on the silicon. At each position, where possible, the Raman signal was measured. A Lorentz was fitted to the Raman spectrum in order to determine the intensity. Since the $TiSi_2$ line is not transparent for visible light, no Raman signal is obtained as long as the laser beam is completely probing the $TiSi_2$. When crossing the edge of the $TiSi_2$ line, the Si signal is detected and increases in intensity until the laser beam is only probing the Si. From the change of the intensity of the Si Raman peak with distance, the diameter of the probing laser beam can be determined. Fig. 6 shows a

typical result of Raman data obtained during a scan across the edge of the $TiSi_2$ line. The 457.9 nm line of the Argon laser was used in these experiments. The intensity of the Si-Raman signal is plotted as a function of the position on the sample. The intensity is zero when probing the silicide, and maximal when probing the Si substrate.

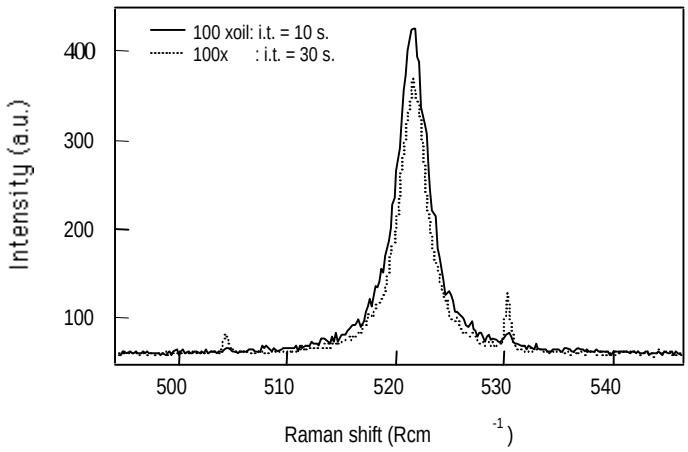

Figure 5 – *Raman signal of silicon obtained with a conventional 100x lens (dotted line, integration time 30 sec) and with an oil immersion 100x objective (dotted line, integration time 10 sec.)*

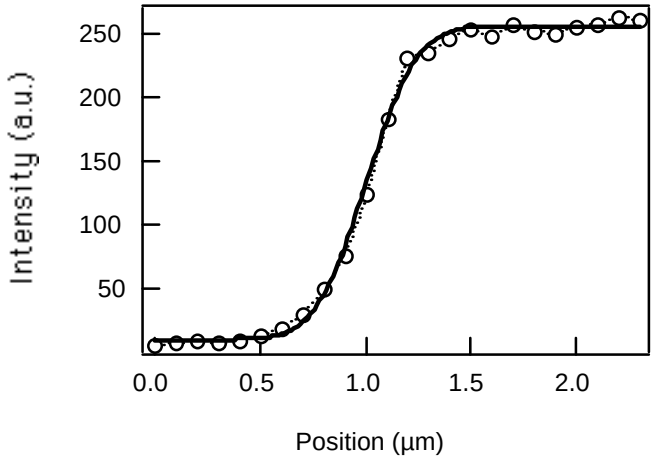

Figure 6 – *Intensity of the Raman signal of silicon obtained during a scan starting on a $TiSi_2$ line and moving to silicon, with an oil immersion 100x lens lens (open symbols). Full line: fit of an integrated Gaussian function to the data.*

In order to determine the spot size in these experiments, a numerical approach of an integrated Gauss function [17] is fitted to the data. The beam diameter was taken as the $1/e^2$ value of this Gauss function. Fig. 6 shows a typical result of such a fit (full line) to the Raman data.

A couple of different lenses and SILs were tested in this way.

A 50x long distance objective (LD), NA = 0.55, could be focused with a SIL underneath due to its large working distance. This lens was used in conjunction with a HSIL and a TSIL. The SILs were made from lapped and polished optical fiber coupling LaSFN9 spherical ball lenses with a diameter of 2 mm. They have a refractive index of 1.877 at a laser light wavelength of 457.9 nm. Also used were a 100x, NA= 0.95 conventional objective and 100x, NA=1.4 oil immersion objective with an n = 1.516 coupling fluid.

3.2 SIL lenses

When putting the HSIL and the TSIL on top of our sample, we obtained in general a smaller intensity of the Raman signal than with the conventional lenses. The smallest spot sizes we could obtain were 0.48 μm and 0.49 μm, respectively, which is better than the obtainable resolution when using the ordinary objectives. However, in most tests the spot size was a little larger and the reproducibility is very poor. A SIL is very hard to use, because its center has to be aligned with both the optical axis and the position on the sample we want to investigate.
If we consider the best spot size of the SILs, we find that the effective NA is almost one (Eq. 1,2). This means that the near-field effect, due to the shorter wavelength in the lens, is not taking place. Although Poweleit [6] does not mention this explicitly, this is the same as found in their Raman experiments with a SIL. It can be explained by taking into account the bottom of the SIL to sample distance, which can easily be more than 0.5 μm due to small particles on the surface, thereby spoiling the enhanced resolution. This also explains the poor efficiency of the Raman signal intensity. A lot of the light is reflected from the bottom of the SIL if it is not coupled to the sample by its evanescent waves. The outer rays in the cone are even totally internally reflected.

3.3 Oil immersion lens, no autofocus

Table I summarizes the results obtained with the conventional 100x lens and an oil immersion lens for two different wavelengths of the laser, but without autofocus.

Table I *- Spot size obtained without autofocus system*

Lens	Wavelength (nm)	Φ (μm) ± sdev	Φ (μm) (Eq.1)
100x, NA = 0.95	514	0.91 ± 0.16 (n = 16)	0.66
	457.9	0.86 ± 0.17 (n = 15)	0.59
100x oil, NA = 1.4	514	0.59 ± 0.01 (n = 8)	0.45
	457.9	0.51 ± 0.04 (n = 5)	0.40

We clearly find a smaller spot size, so, better resolution, for the oil immersion lens. However, there is a large deviation between the theory (Eq. 1) and the experimental results.

3.4 Oil immersion lens, autofocus

The auto-focus system focuses much more precisely than an operator can do by hand, and in addition, it keeps the focus during longer scans: so, the small depth of focus of an oil immersion objective offers no problem. To obtain accurate spot size values, a sample with 10 nm Cr/60 nm Au lines of 1μm wide on a silicon wafer was made at IMEC (figure 7). This sample had a very thin metal layer, which ensured that the metal edge could not induced anomalous optical effects through reflection.

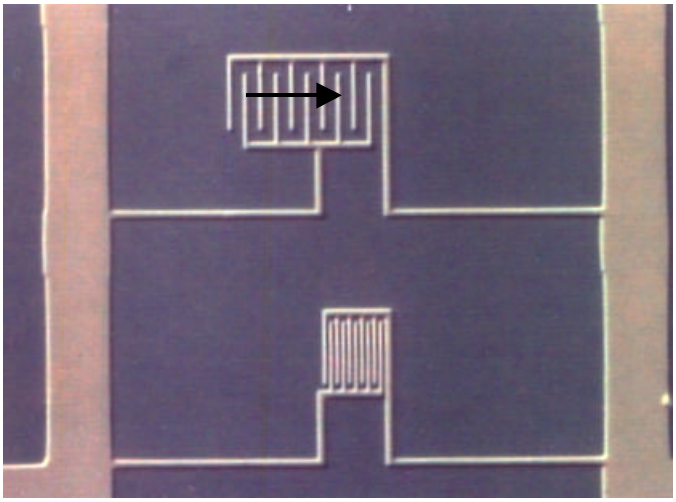

Figure 7 *- Cr/Au sample with scan direction indicated*

Figure 8 shows the results of scans across one 1 µm wide line of this metal film.

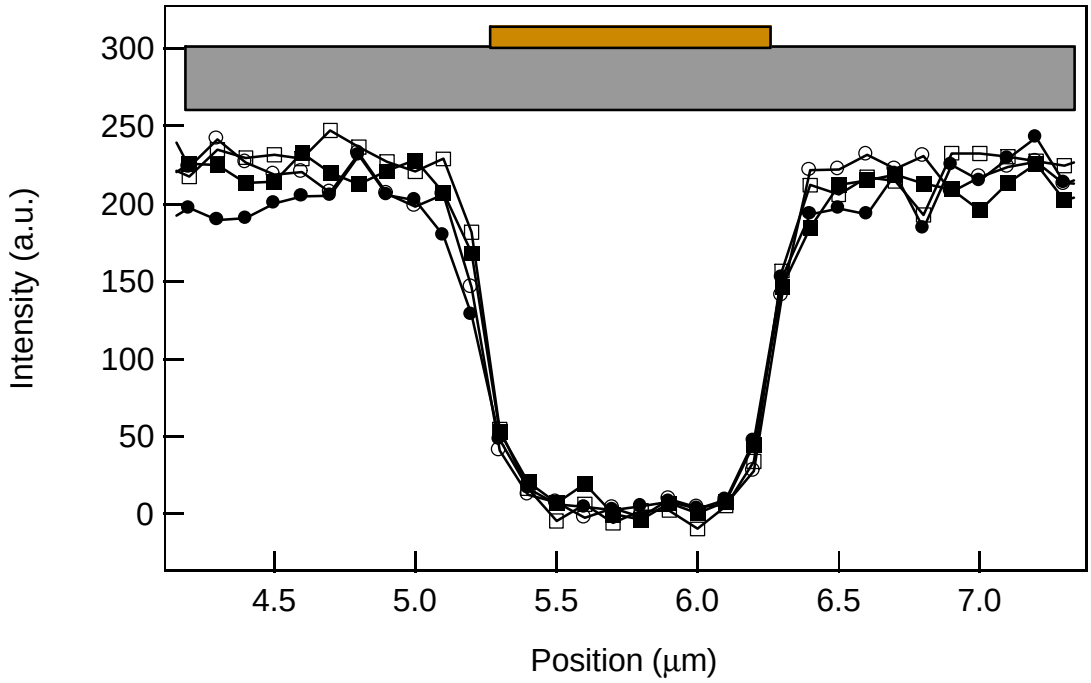

Figure 8 *- Scans with the oil immersion objective + auto-focus over a 1 mm wide Cr/Au line*

In this experiment, we obtained a mean spot size over 8 edge scans of 0.30 µm ± 0.05 µm. This is a very good result, when we realize that Eq. 1 gives us a theoretical obtainable spot size of 0.28 µm at λ = 457.9 nm with our $1/e^2$ intensity criterion. So, a very good agreement between theory and experiment is obtained with this combination of oil immersion lens and auto-focus system.

Table II – *Experimental spot size with oil immersion objective (100x) + autofocus system*

	spot intensity going down	**spot intensity going up**
scan 1	0.41 μm	0.32 μm
scan 2	0.29 μm	0.35 μm
scan 3	0.27 μm	0.26 μm
scan 4	0.28 μm	0.25 μm

An overview of all the different lens combinations and the corresponding theoretical and practical spot sizes is given in Table III for the 457.9 nm line of the argon laser.

Table III – *Spot size, comparison theory and experiment*

objective	**theoretical spot**	**Experimental spot**
100x normal	0.42 μm	0.86 μm ± 0.17 μm
100x normal +auto-focus	0.42 μm	-
50x LD + HSIL	0.39 μm	0.48 μm sometimes
50x LD + TSIL	0.21 μm	0.49 μm sometimes
100x oil immersion	0.28 μm	0.51 μm ± 0.04 μm
100x oil + auto-focus	0.28 μm	0.30 μm ± 0.05 μm

3.5 Discussion

NSOM promises the best spatial resolution in micro-Raman spectroscopy, but, at present, its intensity is too low to perform reliable local mechanical stress measurements. UV-micro-Raman spectroscopy is capable of measuring stress very near the silicon surface, but does not improve spatial resolution due to the lack of really good, high NA UV microscope objectives.
We have seen that an oil immersion lens can reveal details well beyond the resolution of a conventional objective. A solid immersion lens (SIL) is theoretically capable of even a little better spatial resolution, but due to practical problems, there is not much to gain by using a SIL. The invention of a higher NA oil immersion lens (NA= 1.65) [18] will make that the difference in spatial resolution is so small that this can not be a criterion to choose a SIL instead of an oil immersion objective.
An oil immersion objective is much easier to use than a SIL. It can be used just as a conventional objective, but with a little drop of oil between the objective and the sample. The SIL, however, imposes severe restrictions on our measurement variables. Both the surface of the SIL and the sample have to be very clean, so the lens and sample have to be cleaned very well before usage (e. g. ultrasonically). Only in a cleanroom environment there is a small chance that the near-field effect will be significant. It is rather difficult to position the SIL with its center exactly at the optical axis of the microscope objective. Even then, the spot size is less well defined than is the case with an oil immersion objective due to the topography of the sample, because the oil will fill the little spaces between the structures. Using a special kind of SIL with a sharp tip might be advantageous [19].

Of course there are situations in which an oil immersion objective is not usable (cryogenic, high vacuum), but for most of the performed micro-Raman experiments it is the better choice for very high resolution measurements.

4. Deconvolution

4.1 Image theory

Although the optical resolution limit seems unavoidable, there is more information on small details in the image than we immediately see, because information about every detail *is* collected. The blurring of the line scan or image is due to the intensity distribution of the spot, so, if we know the properties of the focused laser spot, we can correct for the introduced faults digitally. This leads us to the field of image theory, and linear image operations in particular.
The point spread function (PSF) gives the *measured image* of a *point of the object*. In our case, the intensity distribution of the laser spot is the PSF. The imaging (blurring) process can be described by a convolution of the sample properties (intensity, mechanical stress, etc.) $f_{prop}(x)$ with the PSF denoted h(x), with x the position [20]. The imaging process also includes additive noise n(x), and the h(x) is assumed to be Gaussian (a reasonable approximation for focused laser beams). Hence we obtain as the image g(x)

$$g_{coll}(x) = f_{prop}(x) * h(x) + n(x) \qquad \text{and} \qquad h(x) \approx e^{-(x-x_1)^2},$$

in which x_1 is the position of the center of the spot and * denotes the convolution integral. For the moment, we ignore the noise. The spot can be moved over the sample in discrete steps only, so we can represent these continuous functions as vectors if we perform a line scan. The object function $f_{prop}(x)$ becomes a vector $\mathbf{f}_{prop,n}$ with n sample points. The PSF can also be regarded as a vector, denoted $\mathbf{h}_m$. The collected vector at the image line $\mathbf{g}_{coll,n}$ is the discrete counterpart of $g_{coll}(x)$. These are the data points we actually measure.

We have to regain the object vector $\mathbf{f}_{prop,n}$ as good as possible from the measured data $\mathbf{g}_{coll,n}$. Therefore, we first look at a basic calculation tool. We can perform a linear image operation on $\mathbf{g}_{coll,n}$, written as

$$\mathbf{i}_n = \mathbf{M}_{n,n}\mathbf{g}_{coll,n},$$

with **M** an n by n operation matrix, which assigns a value to each output vector component **i**[n] according to *all* the input vector components. If this operation does not depend on the position n of the input component, and if it is linear as well, it is the discrete counterpart of the convolution. For component q of the vector **i** we can write

$$\mathbf{i}[q] = \mathbf{h}_{q,n}\mathbf{g}_{coll,n}.$$

In this equation $\mathbf{h}_{q,n}$ is the q^{th} row of the operation matrix **M**. This equation describes how the value of the q^{th} point of a vector **i** can be calculated separately if **i** is a vector which is a convolution of $\mathbf{g}_{coll,n}$ and $\mathbf{h}_n$. This is true both for the image collection (performed by our measurement system), and for the operations we are going to perform to obtain a higher resolution. Now we have a tool to do the inverse of the imaging convolution. We only have to find a matrix **M**, which counteracts the original convolution.
What is the shape of this matrix? We know from the convolution equation that a particular point $\mathbf{g}_{coll}[q]$ at position q on the image line is composed of all components from the object $\mathbf{f}_{prop}$ collected by the equation

$$\mathbf{g}_{coll}[q] = \mathbf{h}_{q,n}\mathbf{f}_{prop,n} ,$$

with $\mathbf{h}_{q,n}$ now the discrete PSF with its center x_1 at q. If we perform this operation for all points on $\mathbf{g}_{coll}$, this is basically a low-pass filter operation. The low frequency components in the image line are left unchanged, because they are much larger than the PSF. The high frequency components, smaller than the PSF, are attenuated by the measurement, because they are smeared out over a couple of vector components. The complementary operation of the low pass filter $\mathbf{h}_{q,n}$ is the high-pass filter $\mathbf{1}-\mathbf{h}_{q,n}$, with **1** the vector which is zero everywhere except for position q, where it is unity.
It attenuates the low frequency components, but leaves the components smaller than the PSF unchanged. Our object consisted of both low-frequency and high-frequency components, so we want the low-frequency components being still in the image, and to remain the same, but we also want the high frequency components to be amplified to such a strength, that the imaging convolution is compensated. This is what we achieve when we combine the original image linearly with its high-pass filtered version, when we do high-emphasis:

$$\mathbf{h}_{high\text{-}emphasis} = \alpha\mathbf{1} + (1 - \alpha)\mathbf{h}_{q,n} .$$

The convolution factor α gives the amount of high-emphasis. When we perform such an operation for each component of the image vector $\mathbf{g}_{coll,n}$, we will approximately regain our original object vector $\mathbf{f}_{prop,n}$. We fill the operation matrix **M** with rows in which the peak of the PSF is moved one step for each succeeding row, like what happened when the spot moved in the original scan. When our vector description of the PSF is very accurate, much of the blurring caused by the PSF can be removed. However, noise will obscure the very high frequency components, which were severely attenuated, so we will never get an exact replica of the original object vector $\mathbf{f}_{prop,n}$. If we overdo this high-emphasis, we introduce a lot of high frequency noise, which will completely obscure our measurement.
Therefore, an optimum value of α exists. For the moment, this value is selected by eye, just by looking at the data for the best result. Obviously, a more objective criterion should be found. The maximum value we can take, and hence the highest improvement in resolution we can obtain, depends on the amplitude and frequency spectrum of the noise in the micro-Raman spectroscopy measurement. Longer integration times will enhance the Raman signal, thereby improving the noise level. However, the measurement time may become prohibitively long, and in addition, due to drift of the optics during the

measurement of one spectrum, the spot size becomes less well-defined, because the setup is only refocused before a spectrum is taken, and not during the spectrum acquisition.

4.2 The algorithm

When we know the size of the laser spot, and assume a Gaussian intensity distribution, the operation matrix **M** can be easily calculated. Because most of this matrix is filled with zero's at the positions where the PSF has an insignificant value, and can become quite large, it is more convenient to calculate the $\mathbf{h}_{q,n}$ for each vector component separately. In conventional image processing, each of the vector components of $\mathbf{g}_{coll,n}$ is just an intensity value. In micro-Raman spectroscopy, each measurement point delivers a complete Raman spectrum. The image operations have to be performed on the complete spectra, to obtain the maximum accuracy. The spectra are saved in a list, in with in each component of the list contains a spectrum. The deconvolution algorithm is applied to all spectra separately. A C++ program was written, which reads in the files containing the spectra, performs the deconvolution with a spot size and convolution factor α given by the user, and then saves the deconvoluted spectra again, for further processing.

4.3 Results and discussion

We applied the algorithm to a measurement on the sample with 10 nm Cr/60 nm Au lines described previously. The experiment was carried out with 50x, NA = 0.75 long distance objective. The results are given in Fig. 7.

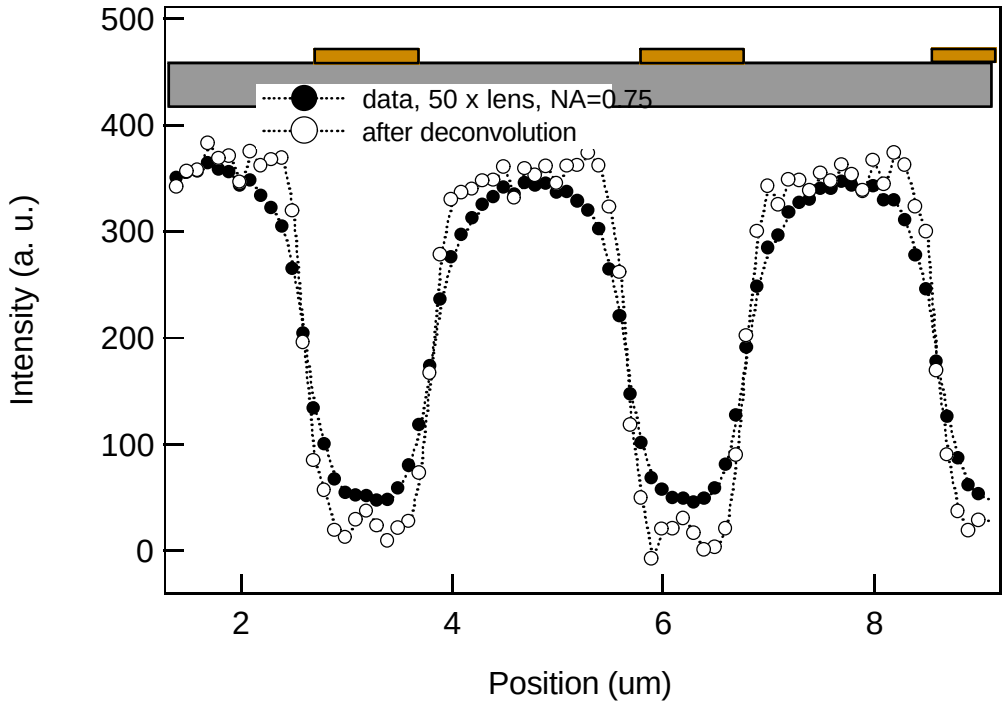

Figure 9 *- Raman data before (full symbols) and after (open symbols) deconvolution.*

We see that the restored versions of the measurement indeed have a higher spatial resolution. Note that the noise is more pronounced, because of the added high frequency components. We also see that in the original 50x measurement the spot was so large, that it could not be completely obscured by the gold lines: the spot is about 1.2 μm, while the lines are only 1.0 μm wide. Therefore, the intensity does not drop completely to zero. In the restored measurement, we see that the intensity of the improved resolution version indeed goes to zero.
More experiments are going on the optimize this deconvolution algoritm. In combination with the oil-immersion objective and the autofocus system, we hope to reach a beam spot of 0.2 μm. Up to now, this algoritm was only applied to Raman intensity data. We expect that this is also useful for stress measurements, because all information concerning the mechanical stress is contained in the intensity data.

4.4 Problems and future possibilities

The main problem with the current approach is the fact that accurate knowledge about the point spread function (PSF) is needed to obtain a reasonable improvement. In real laboratory circumstances the PSF is not so well known, because most samples cannot be used for adequately measuring the spot size. Using a reference sample is no solution, because defocusing for putting our real object under the microscope instead of the reference is already enough to spoil our just determined spot, unless we have an auto-focus system. After a new outlining of the system, we have to measure the spot size again, if we want to use the algorithm.
To solve this, it might be possible to use a blind deconvolution algorithm, which determines the restored image *and* the PSF simultaneously from our data. Although computation times are long because such an algorithm is iterative in nature, the results are hardly worse than the results of its non-blind counterpart. This provides us with the possibility to do a measurement, and automatically deblur the image as a standard procedure. Very impressive results have been achieved with small objects on a black background. In the astronomy it is used often, but the first results in microscopy are also available [21]. One of the problems is to find a criterion on which we can deblur Raman spectra, as ordinary blind deconvolution algorithms use the light intensity to find the deconvolution parameters.

5 Conclusions

The combination of immersion lenses and digital image restoration can improve the spatial resolution of a micro-Raman measurement substantially, from 1 μm to 0.2 μm. A solid immersion lens is theoretically a little better than an oil immersion objective, but practical problems are large. Of course there are measurements in which an oil immersion objective is not usable (cryogenic, high vacuum), but for ordinary micro-Raman spectroscopy with high spatial resolution, it is the better choice.

The best results will be obtained if digital image restoration is used in conjunction with an auto-focused oil immersion objective. The spatial resolution obtained with such a combination is expected to be 0.2 μm ($1/e^2$ intensity). This is the best resolution, which can reasonably be obtained for quantitative local mechanical stress measurements using micro-Raman spectroscopy.

Further experiments will be performed in the frame of STREAM to test the above conclusions further:

- experiments with different lenses (100x, 50x, 10x) to see whether the deconvolution algoritm can, in a correct way, predict the stress as measured with the 100x by using data from the 50x lens, and, in the same way, from the 10x to the 50x
- experiments on the test structure of Fig. 7 with 100x oil objective + autofocus + deconvolution to confirm that a 0.2 μm beam spot can be obtained
- experiments on the STI structures with 100x oil objective + autofocus + deconvolution for comparison with CBED
- experiment with a UV-Raman instrument to see whether resolution can be improved with that instrument

In addition, a journal paper will be published reporting on these results.

References

1. Duncan W., J. Vac. Sci. Tech. A 14(3), pp.1914-1918, 1995
2. Webster S., D.N. Batchelder, and D.A. Smith. Appl. Phys. Lett. **72**(12), pp. 1478-1480, 1998
3. Grausem J., B. Humbert, A. Burneau and J. Oswalt, Appl. Phys. Lett. **70**(13), pp. 1671-1673, 1997
4. Zeisel D., B. Dutoit, V. Deckert. T. Roth and R. Zenobi. Anal. Chem. **69**, pp. 749-754, 1997
5. Dombrowski, K., I. De Wolf and B. Dietrich, Appl. Phys. Lett. 75 (16) 1999, p.2450
6. Poweleit, C. D., A. Gunther and S. Goodnick and J. Menendez, Appl. Phys. Lett., 73 (16), 1998, p. 2275
7. Terris B.D., H.J. Martin and D. Ruger, Appl. Phys. Lett. **68**(2), pp. 141-143, 1996
8. Ghislain L.P. and V.B. Elings Appl. Phys. Lett. **72**(22), pp. 2779-2781, 1998
9. Yoshita M., T. Sasaki, M. Baba and H. Akiyama Appl. Phys. Lett. **73**(5), pp. 635-637, 1998
10. Born, M. A. and E. Wolf, *Principles of optics*, 4th ed., Pergamon press , Oxford, 1970
11. Hecht, E., *Optics*, 2nd ed. , Addison-Wesley Publishing Company, New York, 1987
12. Jodoin, R. E., *Diffraction of a laser beam*, Am. J. Phys. 47 (6), 1979, p. 498
13. De Wolf I., Semicond. Sci. Technol. **11**, 19, 1996
14. De Wolf, I., J. Chen, M. Rasras, W. M. van Spengen and V. Simons, Proc. of the SPIE, Vol. 3897, 1999, p. 239.

15. Sasaki, T., M. Baba, M. Yoshita, H. Akiyama, Application of a solid immersion lens to high-resolution photoluminescence imaging of patterned GaAs quantum wells, Jpn. J. Appl. Phys., 36, p. L962, 1997
16. van Spengen W. M., *Possibilities in failure analysis using a micro-Raman spectroscopy measurement system,* M. S. Thesis, Eindhoven University of Technology, The Netherlands, 1999.
17. Abramowitz, M. , Handbook of mathematical functions, 9th ed. , Dover publications, New York 1972
18. Caldwell, B. J., *Ultra high NA microscope objective*, Optics & Photonics News, 44, 44 (Nov. 1997)
19. Ghislain, L. P. and V. B. Elings, *Near-field scanning solid immersion microscope*, Appl. Phys. Lett,, 72 (22), 1998, p. 2779
20. van der Heijden, F., John Wiley & Sons Ltd., Chichester, 1994
21. Krishnamurthi, V., L. Yi-Hwa, S. Bhattacharyya, J. N. Turner, T. J. Holmes, Appl. Opt., Vol. 34, No. 29, 1995, p. 6633